Briefings in Bioinformatics, 2025, **26(3)**, bbaf163
https://doi.org/10.1093/bib/bbaf163
Case Study

Metabolism-associated protein network constructing and host-directed anti-influenza drug repurposing

Hao Tang[1,‡], Feng Jiang[1,‡], Zhi Zhang[1], Jiaojiao Yang[2,3], Lu Li[2,3,4], Qingye Zhang[1,*]

[1]Hubei Key Laboratory of Agricultural Bioinformatics, College of Informatics, Huazhong Agricultural University, Shizishan Street 1, Wuhan, 430070 Hubei, China
[2]National Key Laboratory of Agricultural Microbiology, College of Veterinary Medicine, Huazhong Agricultural University, Shizishan Street 1, Wuhan, 430070 Hubei, China
[3]Key Laboratory of Preventive Veterinary Medicine in Hubei Province, The Cooperative Innovation Center for Sustainable Pig Production, Shizishan Street 1, Wuhan, 430070 Hubei, China
[4]International Research Center for Animal Disease, Ministry of Science and Technology of the People's Republic of China, Shizishan Street 1, Wuhan, 430070 Hubei, China
[*]Corresponding author. Hubei Key Laboratory of Agricultural Bioinformatics, College of Informatics, Huazhong Agricultural University, Shizishan Street 1, Wuhan, 430070 Hubei, China. E-mail: zqy@mail.hzau.edu.cn
[‡]Hao Tang and Feng Jiang contributed equally to this work.

Abstract

Host-directed antivirals offer a promising strategy for addressing the challenge of viral resistance. Virus–host interactions often trigger stage-specific metabolic reprogramming in the host, and the causal links between these interactions and virus-induced metabolic changes provide valuable insights for identifying host targets. In this study, we present a workflow for repurposing host-directed antivirals using virus-induced protein networks. These networks capture the dynamic progression of viral infection by integrating host proteins directly interacting with the virus and enzymes associated with significantly altered metabolic fluxes, identified through dual-species genome-scale metabolic models. This approach reveals numerous hub nodes as potential host targets. As a case study, 50 approved drugs with potential anti-influenza virus A (IVA) activity were identified through eight stage-specific IVA-induced protein networks, each comprising 699–899 hub nodes. Lisinopril, saxagliptin, and gliclazide were further validated for anti-IVA efficacy *in vitro* through assays measuring the inhibition of cytopathic effects and viral titers in A549 cells infected with IVA PR8. This workflow paves the way for the rapid repurposing of host-directed antivirals.

Keywords: metabolic reprogramming; host-directed antivirals; genome-scale metabolic models; protein–protein interaction networks; influenza virus–host interactions

Introduction

Viral infections continue to pose a serious threat to global public health due to their high transmissibility, high lethality, and severe sequelae. The rapid development of viral resistance to antiviral drugs [1–3], coupled with the environmental toxicity of broad-spectrum antivirals [4], poses significant challenges to the use of small molecules targeting viral antigens. Host-directed strategies are applicable not only to noninfectious diseases [5–7] but also to antiviral therapies [8]. The high conservation of host molecules in evolution suggests that host-directed antivirals can maintain long-term effectiveness. Most host-directed antiviral small molecules can exert immunomodulation and inflammation regulation by targeting host proteins [9], or affect conserved virus–host interaction patterns at the cell surface [10] or intracellularly [11], thereby providing effective protection against viral infection. The latter essentially disrupts the transmission of infection signals from the viral particles to the host cells. Developing drugs based on interspecies molecular interactions and signaling can directly link drug actions to the virus lifecycle [12], which may aid in elucidating the antiviral mechanisms of drugs. However, the implementation of this strategy heavily relies on exploring the relevance of virus–host interaction patterns and downstream responses that include metabolism.

Driving metabolic reprogramming stands as a primary survival strategy employed by most viruses, beneficial for their adaptation to the host environment [13–15]. The molecular interactions between viruses and hosts contribute to the aforementioned metabolic alterations. Among them, many instances of virus-induced metabolic reprogramming can be achieved solely through direct interactions either between viral proteins and host proteins or between host proteins themselves. For example, the K1 protein of Kaposi's sarcoma–associated herpesvirus (KSHV), which binds to and activates 5′ adenosine monophosphate-activated protein kinase (AMPK) [16], regulates the catalytic activities of HMG-CoA reductase [17] and glycogen synthases (GYS1) [18, 19] by binding to and phosphorylating these enzymes. The oncogenic protein E6 of human papillomavirus (HPV), which binds to the human protein E6AP, recruits and induces the ubiquitin-dependent degradation of the human tumor suppressor protein p53 [20, 21], a protein that binds to and inhibits the activity of glucose-6-phosphate dehydrogenase (G6PD) [22]. In addition, multiple viral proteins regulate specific metabolic reactions

Received: October 4, 2024. **Revised:** March 5, 2025. **Accepted:** March 23, 2025

through direct binding to host metabolic enzymes [23–26]. These human proteins, which first interact with viral molecules, transmit reprogramming signals to metabolic enzymes through direct protein–protein interactions or directly alter the metabolic profile. So, systematically exploring infection-induced metabolic disturbances will aid in identifying virus-dependent host targets.

Protein–protein interaction networks (PPINs) serve as repositories of molecular knowledge within cells, crucial for unraveling intricate biological causality and identifying disease targets. Current strategies for target identification and drug development based on PPINs have achieved notable success. Mosharaf *et al.* identify potential targets by constructing a delirium-associated PPIN [27]. The ProGENI algorithm leverages large-scale biological networks with protein–protein interactions (PPIs), along with basal gene expression and drug response data, to predict targets related to cancer drug responses [28]. NETTAG, a network-based deep learning framework, integrates multi-omics data and PPINs to identify potential risk genes and relative drugs for Alzheimer's disease [29]. Han *et al.* constructs coronavirus-induced PPINs using infection-related differentially expressed genes for target identification and anti-infective drug repurposing [30]. However, these strategies struggle to elucidate the relationship between targets and viral infection–associated metabolic reprogramming. Given that metabolic disturbances are a common outcome of viral infections [31], utilizing PPINs to infer causal relationships between host proteins that interacted with virus and metabolic enzymes responsible for differential reaction rates (flux) contributes to exploring viral pathogenic mechanisms. To this end, host proteins directly interacting with the virus and key enzymes responsible for differential reaction rates (flux) can be hypothesized as 'causal' nodes and 'consequential' nodes, respectively, during the aforementioned metabolic reprogramming. These causal and consequential nodes were associated by PPINs to generate a layered network with potential signaling transduction patterns, which contributes to exploring host targets.

Exploring host metabolic changes provides insights into the pathogenic process [32]. The genome-scale metabolic model (GSMM), as a platform that showcases the relationships between metabolic reactions and metabolites within a species [33], is employed to identify virus-modulated metabolic reactions and associated enzymes (consequential nodes). This approach has been extensively used to study the pathogenic mechanisms of various viruses, including coronaviruses [34, 35]. Furthermore, integrating the viral proliferation process as an additional biomass equation within host metabolic models allows for a detailed understanding of how viruses impose metabolic burdens on infected cells, accurately predicting metabolic changes [34, 35]. Ultimately, key enzymes responsible for differential fluxes, regarded as consequential nodes, were linked with causal nodes of interactions to allow for inferring rich regulatory relationships, which help uncover the dynamic changes and mechanisms of virus-induced host metabolism. Therefore, the induced networks derived from key metabolic enzymes provide a convenient approach for the development of host-directed antivirus effecting potential signaling or metabolic states in patients, such as those infected with the influenza virus. Influenza remains a formidable global public health challenge due to its high infectivity and pathogenicity [36]. Dysregulated immune responses and associated complications contribute significantly to the elevated mortality rates observed in severe cases of influenza [37]. To alleviate the pressure from rapid drug-resistant strain emergence, there is a necessity to explore the antiviral capabilities of existing drugs.

The study utilized infection stage–specific dual-species GSMMs, integrated with IVA biomass equations (IVBOEs) and constrained by *in vivo* and *in vitro* infection transcriptomes, to characterize metabolic changes during infection and identify Enzymes responsible for Reactions with significantly different Fluxes (ERFs, consequential nodes). ERFs were associated with Host proteins Directly Interacting with influenza virus Proteins (HDIPs, causal nodes) to generate IVA-induced protein networks (IVIPNs). This strategy for generating IVIPNs that associate metabolism with viral interactions differs from previous virus–host protein interaction networks [38–40]. The network analysis to condition-specific IVIPNs implied disease-related hub nodes that facilitated repurposing of anti-IVA drugs via network proximity. This study highlights drug development based on disease-induced protein networks will offer new insights into treating viral diseases and elucidating their pathogenic mechanisms.

Results

To explore host-directed antiviral drugs guided by interspecies interactions and metabolic reprogramming correlations, this study introduced a workflow that constructed a protein interaction subnetwork connecting HDIPs with ERFs derived from dual-species GSMMs to identify infection-related host proteins. Key members of these host proteins were employed for drug repurposing and efficacy assessment in host-directed antiviral therapies against influenza (Fig. 1).

The genome-scale metabolic models integrated with influenza virus A biomass equation possess more metabolic details

To characterize IVA-induced metabolic disturbances, dual-species GSMMs containing the IVA biomass equation (IVBOE) were first constructed. The proliferation of IVA in host cells was represented by an additional biomass equation in the host GSMMs. The IVBOE simulated the molecular composition of proteins, nucleic acids, and lipids of IVA particles by using stoichiometric coefficients. The contribution of nucleotides to IVBOE was determined by the influenza virus genome sequence and replicative intermediates, with the calculation of the latter's nucleotide composition requiring influenza virus translation efficiencies (TEs) (Fig. 2A and B, Source Data S1 and S2). Amino acid contributions depended on their compositions in each protein and related protein copy numbers (Fig. 2C, Source Data S2). Lipid contributions refer to the lipid content of the Golgi membrane in host cells [34, 41] (Fig. 2D, Source Data S2). The consumption of amino acids, nucleotides, lipids, and energy molecule adenosine triphosphate (ATP), along with the release of pyrophosphate, constituted the biomass equation IVBOE (Source Data S2).

To demonstrate the enhanced predictive capability of IVBOE integration, the numbers of essential metabolic reactions and reactions with differential fluxes were compared between integrated and non-integrated IVBOE GSMMs. Essential reactions were extracted from GSMMs using the task-driven ftINIT algorithm for tissue-specific model reconstruction [42]. This algorithm, along with a time-series transcriptomic dataset from IVA-infected and uninfected HTBE cells (five time points) [43](Data ref: Heinz, Texari *et al.*, 2018), constrained both integrated IVBOE GSMMs and their non-integrated counterparts, resulting in a total of 20 GSMMs. Comparison revealed that integrated GSMMs (IVBOEmodels) captured more essential reactions 18–24 hpi compared to untreated infection GSMMs (UImodels) (Fig. 2E, Source Data S6). Differential flux analysis further demonstrated that IVBOEmodels exhibited significantly more reactions with differential flux than UImodels (Fig. 2F-J, Source Data S6). Additionally, except for the hpi 24-h IVBOEmodel, a higher

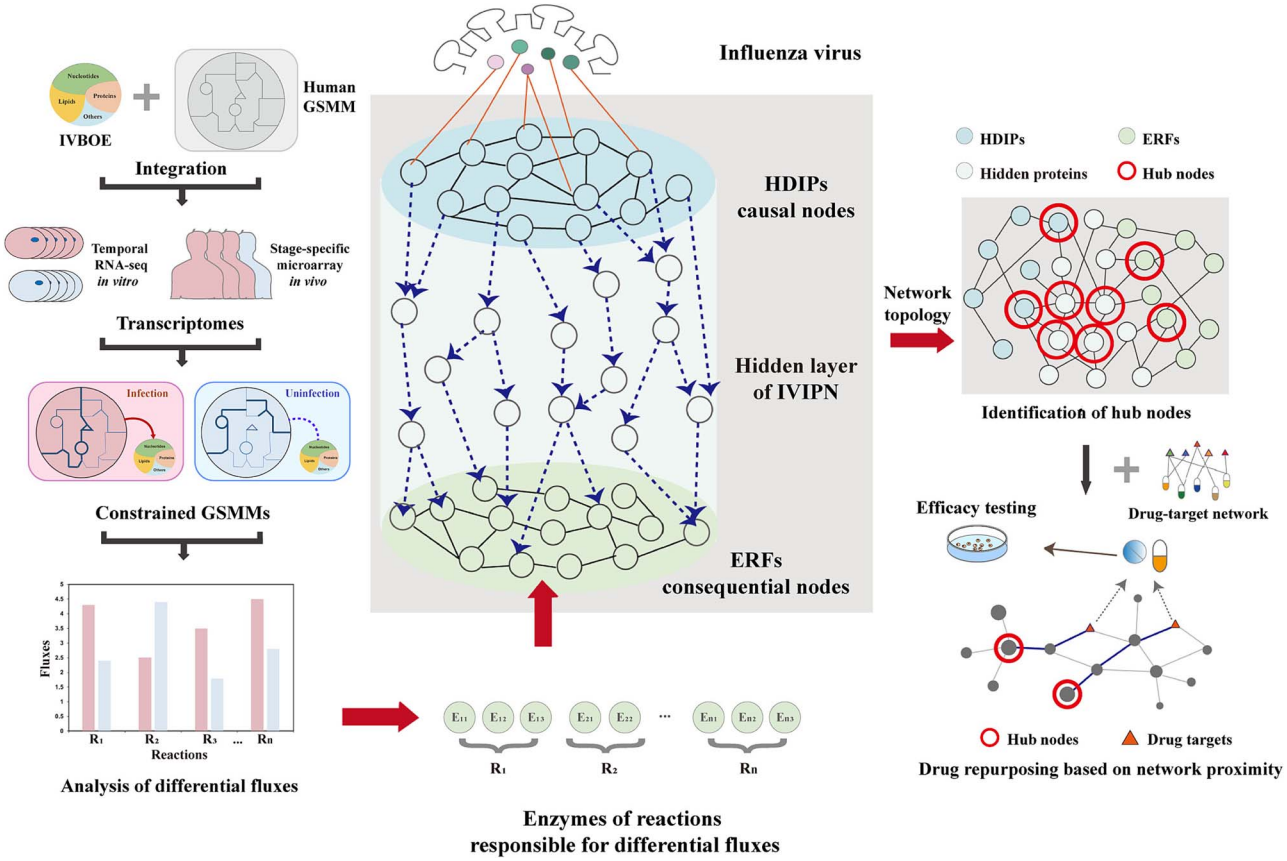

Figure 1. The construction and application of IVA-induced protein networks (IVIPNs). Human genome-scale metabolic models (GSMMs) incorporating influenza virus biomass equation (IVBOE) were constrained by transcriptomes from temporally infected cells or from patients at different infection stages to predict enzymes responsible for reactions with significantly differential fluxes (ERFs, as "consequences"). These enzymes were concatenated with known host proteins directly interacting with influenza virus proteins (HDIPs, as "causes") to obtain multiple condition-specific IVIPNs. IVIPNs associated with late-stage or severe infections were subsequently used to guide the repurposing and efficacy identification of host-directed anti-IVA drugs.

Table 1. The ratio of key genes related to influenza virus infection in the genes responsible for differential flux reactions (%).

Time (h)	IVBOFmodels	UImodels
3	81.4 (136/167)	81.0 (94/116)
6	82.3 (144/175)	81.8 (121/148)
12	83.2 (139/167)	81.6 (125/153)
18	80.6 (133/165)	78.3 (65/83)
24	80.1 (117/146)	80.8 (118/146)

proportion of genes responsible for differential flux reactions were associated with crucial genes related to influenza virus infection (see Materials and Methods) (Table 1, Source Data S7). Thus, the integration of IVBOE enhances the sensitivity of GSMMs to capture key host factors involved in virus-induced metabolic changes, facilitating the precise identification of key enzymes responsible for metabolic reprogramming.

Specific metabolic differences post-influenza virus A infection are captured by IVBOEmodels

IVBOEmodels were employed for differential flux analysis to discovery host metabolic reprogramming induced by IVA infection. Transcriptomic data from IVA-infected and uninfected HTBE cells (five time points) were used to constrain 10 IVBOEmodels. The reactions with differential fluxes (Source Data S3) identified by pairwise analysis were enriched in various metabolic subsystems. Metabolic fluctuations were notable in subsystems related to the "carnitine shuttle (mitochondrial)," "transport reactions," and "nucleotide metabolism" throughout all infection stages (Fig. 3A, Source Data S3). "Pyrimidine metabolism," "tricarboxylic acid cycle and glyoxylate," and "glycolysis/gluconeogenesis" were disrupted early in the infection, while "biopterin metabolism" showed more severe flux changes in later stages. Reduced flux in the carnitine shuttle was linked to the influenza virus utilizing host long-chain fatty acids for lipid membrane synthesis [44]. Decreased flux in the biopterin pathway has been observed in patients with hepatitis E and rabies virus infections [45, 46].

IVBOEmodels, constrained by transcriptomic data from whole blood samples of influenza patients at different infection stages (three stages) [47] (Data ref: Dunning *et al.*, 2018), were employed for comparative analysis. Metabolic state differences between patients with varying infection levels and healthy individuals were observed (Fig. 3B, Source Data S3), reflecting similar metabolic changes seen in HTBE cells pre- and postinfection. Additionally, infection impacted metabolic fluxes in "folate metabolism," "C5-branched dibasic acid metabolism," "arginine and proline metabolism," and "pentose and glucuronate interconversions."

In summary, specific flux analyses *in vitro* and *in vivo* identified metabolic disturbances effected by influenza virus biomass, providing critical consequential nodes for IVIPN construction.

Construction of influenza virus A–induced protein networks

The key enzyme composition in stage-specific metabolic networks can derive stage-specific induced protein networks IVIPNs that are associated with virus–host interactions and metabolic

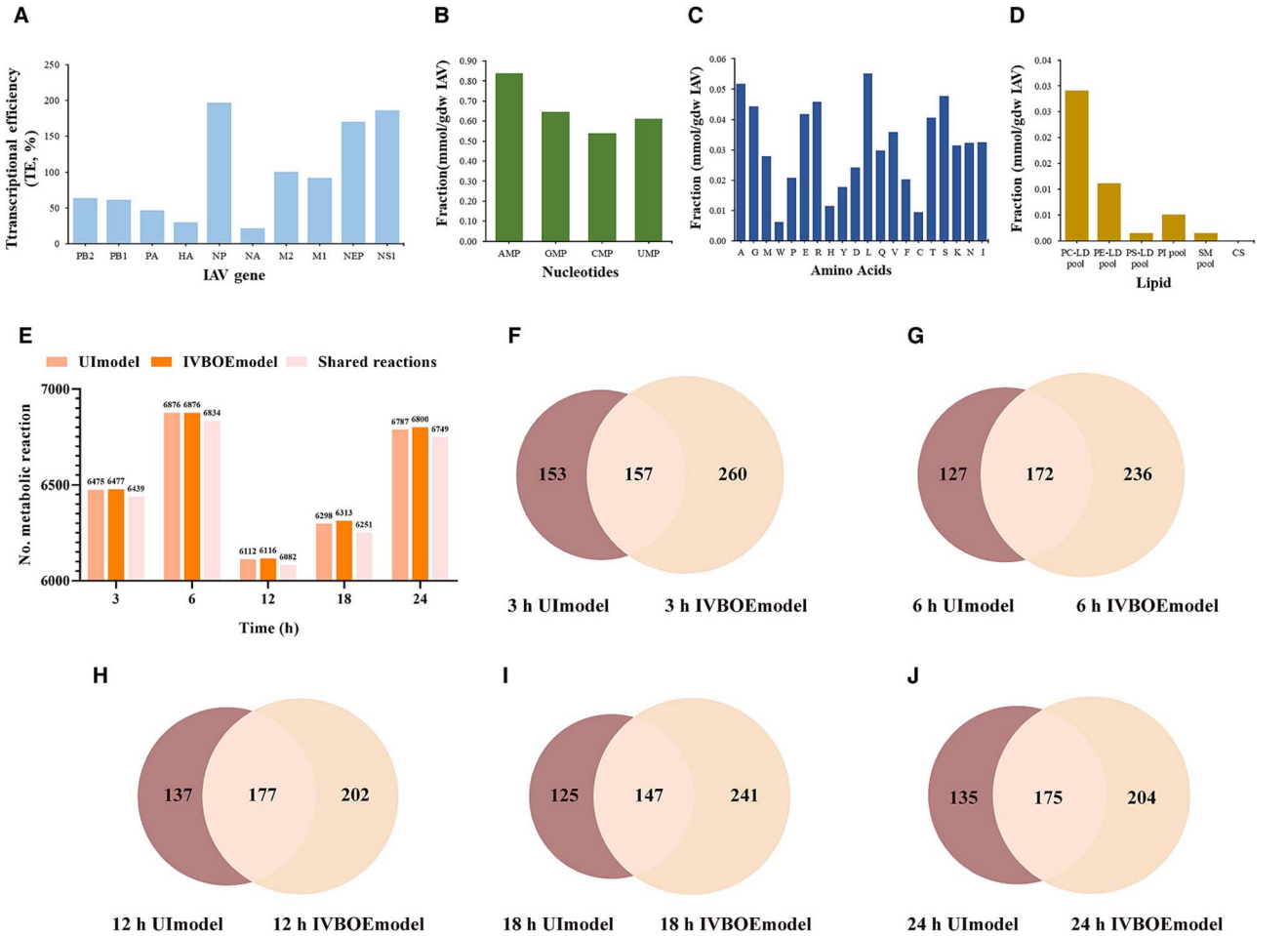

Figure 2. The formation of IVBOE and differences in model structure and predictive performance between IVBOEmodels and UImodels. (A) Translation efficiencies (TEs) of IVA genes. TEs were calculated from influenza virus–host interaction transcriptomes and ribosome footprints. The mole composition of nucleotides (B), amino acids (C), and lipids (D) in IVBOE. Composition of total essential reactions (E) and reactions responsible for differential fluxes (F–J) in temporal IVBOEmodels and UImodels. Temporal GSMMs were constructed by integrating RNA-seq data from HTBE cell samples infected with the influenza virus via the ftINIT algorithm. Prediction of reaction fluxes and extraction of reactions with differential fluxes were achieved through flux sampling and Kolmogorov–Smirnov (KS) test.

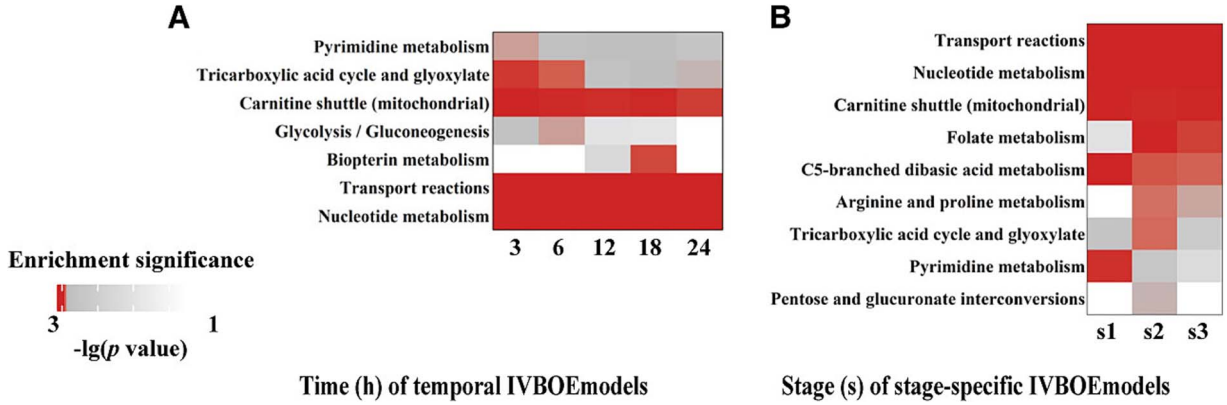

Figure 3. Condition-specific differential metabolic subsystems. Temporal metabolic differences in HTBE cells infected with influenza virus (five time points) (A) and stage-specific differences in influenza patients (three stages) (B), inferred through differential flux analysis of constrained IVBOEmodels. Prediction of reaction flux values and extraction of reactions with differential fluxes were achieved with flux sampling and KS test. Subsystems with $-\lg(p) > 1.301$ were considered significantly enriched by hypergeometric test.

reprogramming. The involvement of metabolic enzymes, rather than differentially expressed genes [30], can provide more unequivocal causal relationships in regulating metabolism. Each IVIPN (Source Data S4) consists of three components (Fig. 4A): (i) Host proteins Directly interacting with Influenza virus Proteins (HDIPs, causal nodes); (ii) Enzymes responsible for Reactions with significantly differential Fluxes (ERFs, consequential nodes); and (iii) protein pathways connecting HDIPs and ERFs via the

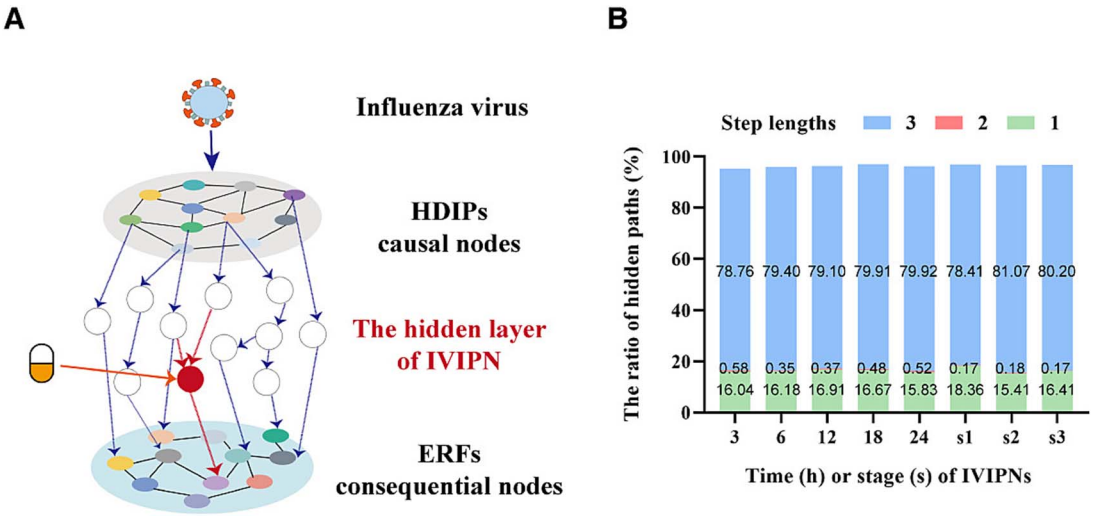

Figure 4. The construction of IVIPN. (A) Structural hierarchy of IVIPN, where hidden layer was obtained via Dijkstra algorithm. (B) Statistical analysis of step lengths of hidden paths in five temporal and three stage-specific IVIPNs. HDIPs, host proteins directly interacting with influenza virus proteins; ERFs, enzymes responsible for reactions with significantly different fluxes.

shortest steps (hidden layer). A total of five time-series and three stage-specific IVIPNs were derived from condition-specific consequential nodes. Each of the eight IVIPNs contained 14 298–14 734 nodes with 510 562–547 570 edges. The hidden layer of each IVIPN consisted of 5349–8300 unique proteins. Approximately 78% of the pathways in these hidden layers comprised more than three proteins (Fig. 4B, Source Data S4). The IVIPNs established via this strategy aimed to encompass potential signaling patterns that were strongly associated causal nodes with consequential nodes.

influenza virus A–induced protein networks are enriched with specific hub nodes relevant to influenza virus A infection

The hub nodes in IVIPNs, as intersections of multiple pathways within the cell, constitute essential biological modules and potential host targets [48]. To validate virological significance of hidden layers, four network topology algorithms were applied to identify hub nodes related to viral infection within each hidden layer. Each of the eight IVIPNs contained 699–899 unique hub nodes, with at least 67% in each hidden layer. Kyoto Encyclopedia of Genes and Genomes (KEGG) pathway enrichment analysis revealed that hub nodes in each hidden layer were significantly associated with terms such as "viral carcinogenesis," "human immunodeficiency virus 1 infection," "human cytomegalovirus infection," and "hepatitis B" ($q < 0.05$) (Table S2). These results demonstrate the validity of the hidden layer for inferring influenza pathogenic mechanisms.

Reasonable hidden layers constitute the main part of IVIPNs and provide an abundance of hub nodes and edges. The characteristics of hub node variations in IVIPNs determine the stage-specific impact of viral infection on host pathways. To investigate the specific host molecular mechanisms relied upon by IVA infection at different stages, unique hub nodes from the temporal IVIPNs were extracted via four network analysis methods for Gene Ontology (GO) enrichment (Fig. 5A, Source Data S5). The significant enrichments of pathway "viral genome replication" at 3 hpi, as well as "extrinsic apoptotic signaling pathway" and "regulation of leukocyte mediated immunity" at 6 hpi, were supported by previous studies [49, 50]. Additionally, enrichment in "negative regulation of sodium ion transmembrane" confirmed the initial downregulation of ion channel expression and activity in host epithelial cells during influenza infection [51].

The specific significant enrichment with evidence was observed primarily in "organelle membrane fusion" at 18 hpi, "ribonucleoprotein complex subunit organization" at 24 hpi, and "protein autoubiquitination" during 18–24 h. The functionality associated with "organelle membrane fusion" ensured that the influenza virus, which relies on endocytosis for cellular entry, can fuse with endosomal membranes, thereby trafficking RNP into the cytoplasm [52]. "Ribonucleoprotein complex subunit organization" and "protein autoubiquitination" supported the translation and post-translational modification of viral proteins [53, 54]. Ubiquitination of the influenza virus polymerase contributes to the enhancement of its activity [54].

Furthermore, enrichment of unique hub nodes associated with three different infection stages revealed that pathways in stages 2 and 3 resemble those observed in later stages of *in vitro* infection (Fig. 5B, Source Data S5). Inflammatory pathways, including "intrinsic apoptotic signaling pathway" and "cell death in response to oxidative stress," were also significantly enriched with evidence [55, 56].

Overall, these findings underscore the ability of IVIPNs to accurately capture the developmental dynamics of IVA infection. These centrally important nodes, essential for virus dependence, could potentially guide host-directed therapeutic strategies.

Effective anti-influenza virus A drugs identified via repurposing based on severe influenza virus A–induced protein networks

The interactions between drugs and host targets suggested the potential to interfere with the IVA infection process by targeting hub nodes. Considering that the differences of cell sample sources or cell lines determine the variation in the composition of hub nodes, hub nodes extracted from IVIPNs generated from *in vitro* late-infection (24 hpi) and *in vivo* severe infection (s3) samples were both utilized for drug repurposing. A total of 4428 small molecules with drug–target relationships from the DrugBank database (updated as of 4 January 2023) [57] were applied to repurpose via a network-based proximity analysis [58]. Thus, a total of 34 and 16 FDA-approved drugs were identified based on networks generated from *in vitro* and *in vivo* samples, respectively, each supported by established antiviral evidence (Table S3). Notably, three candidates (salmeterol, ruxolitinib, and vemurafenib) of the 34 drugs and two candidates (minocycline

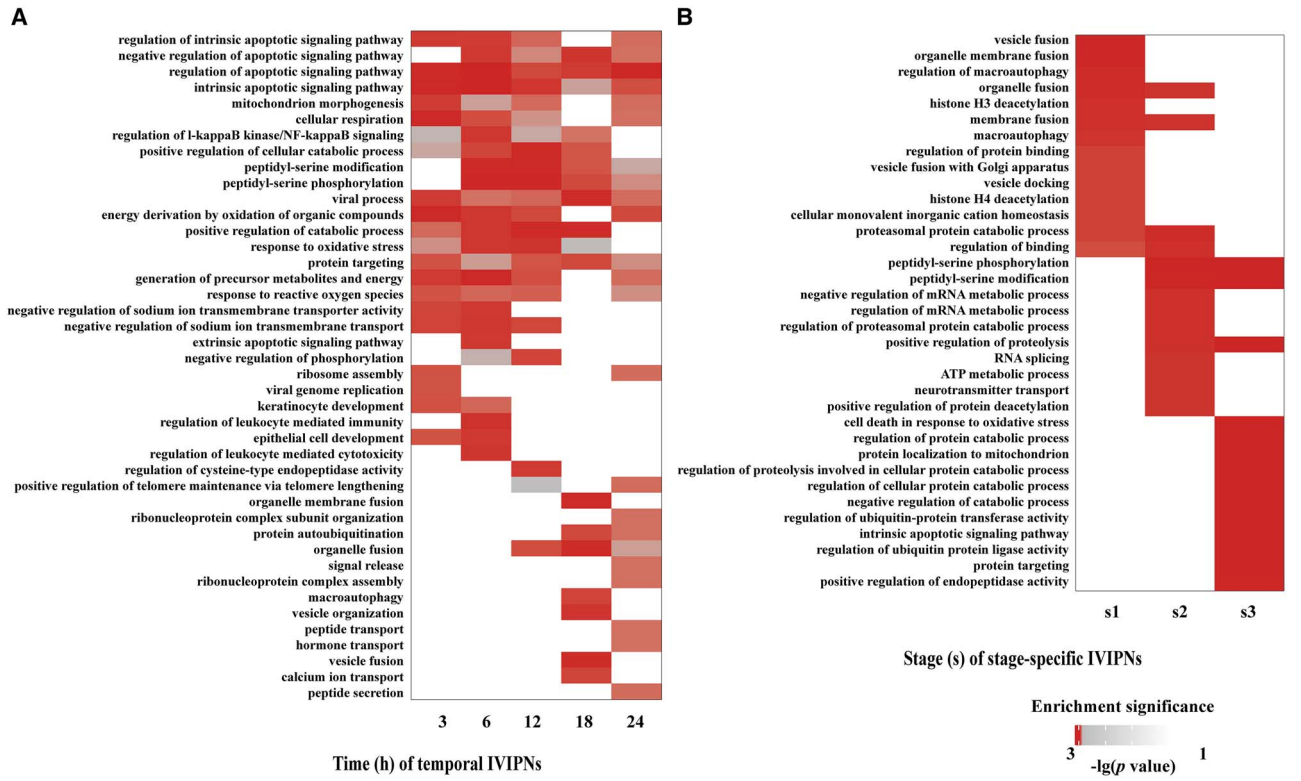

Figure 5. The GO enrichment of unique hub nodes in IVIPNs. Hub nodes of five temporal (A) and three stage-specific IVIPNs (B) were identified through eigenvector centrality, degree centrality, betweenness centrality, and restart random walk. Pathways with $-\lg(p) > 1.301$ as significantly enriched.

and dipyridamole) of the 16 drugs possessed known host-directed anti-IVA effects.

Based on assessment of drug availability and structural uniqueness, an additional five candidates lacking antiviral evidence (saxagliptin, lisinopril, gliclazide, sorafenib, and ezetimibe) screened from *in vitro* and *in vivo* samples were evaluated for their anti-IVA capacities by *in vitro* assay of cytotoxicity, with inhibition of cytopathic effects and virus titers (Fig. 6, Source Data S8). A549 cells infected with PR8 H1N1 virus were used as the model system. Vemurafenib and oseltamivir served as positive controls targeting host and IVA, respectively. The results indicated that these five drugs possessed varying degrees of ability to inhibit cytopathic effects (Fig. 6), as saxagliptin showed dose-dependent inhibition of cytopathic effect within the range of 150–400 μM (middle of Fig. 6C). Sorafenib and ezetimibe inhibited cytopathic effects within the lower range of 0.75–6.25 μM without cytotoxicity (middle of Fig. 6F and G). Additionally, 100 μM lisinopril demonstrated anti-IVA potency similar to that of 50 μM vemurafenib (bottom of Fig. 6A and D). In addition, 300 μM gliclazide inhibited half of the virus titers compared with untreated group (bottom of Fig. 6E). These results indicate the hub node-based screening can identify effective anti-IVA drugs. Moreover, the interaction patterns between effective drugs and host proteins may provide insights into identifying host targets and exploring the pathogenic mechanisms of IVA.

Discussion

The efficacy of antiviral drugs is challenged by the rapid mutation of viruses [1–3]. Given the strict dependence of viral replication on host activities, targeting host factors provides an alternative antiviral strategy [12]. Initially, viruses invade by interacting with host molecules and subsequently induce metabolic reprogramming in host cells, diverting energy and resources to synthesize viral components. However, the complexity of viral hijacking mechanisms impedes the understanding of viral disease progression. This study investigated the IVA infection–induced characteristics by constructing an infection-induced protein network (IVIPN), linking virus-host interactions (causal layer) to changes in the host metabolic profile (consequential layer). To simulate the post-hijacking metabolic landscape, IVBOE, based on influenza virus biomolecular data, was integrated into human GSMMs to generate IVBOEmodels. Transcriptomic data incorporation aimed to accurately reflect metabolic alterations post-hijacking. Differential flux analysis of the IVBOEmodels identified the consequential layer in IVIPNs. Condition-specific IVIPNs were used to precisely identify hub nodes contributing to influenza infection and for drug repurposing.

Considering only direct interactions between drugs and hub nodes can lead to the omission of indirect interaction information. Additionally, the multitarget nature of drugs complicates the analysis of interaction outcomes. Therefore, network proximity was employed to predict drugs topologically closest to multiple hub nodes. The five drugs identified and screened for anti-IVA activity also possess antiviral effects against other viruses (Table S3). The efficiency of this screening suggests that the anti-infection effects may be associated with host factors directly or indirectly interfered with by the drugs. For instance, serine/threonine kinase BRAF (NCBI Gene ID: 673), a target of sorafenib, is part of the Raf/MEK/ERK signaling cascade crucial for IVA replication [59, 60], suggesting the inhibition to BRAF might contribute to the anti-IVA effect of sorafenib. Vascular endothelial growth factor A (VEGFA, NCBI Gene ID: 7422), targeted by gliclazide, is associated with kidney injury in H1N1 influenza patients [61, 62]. However,

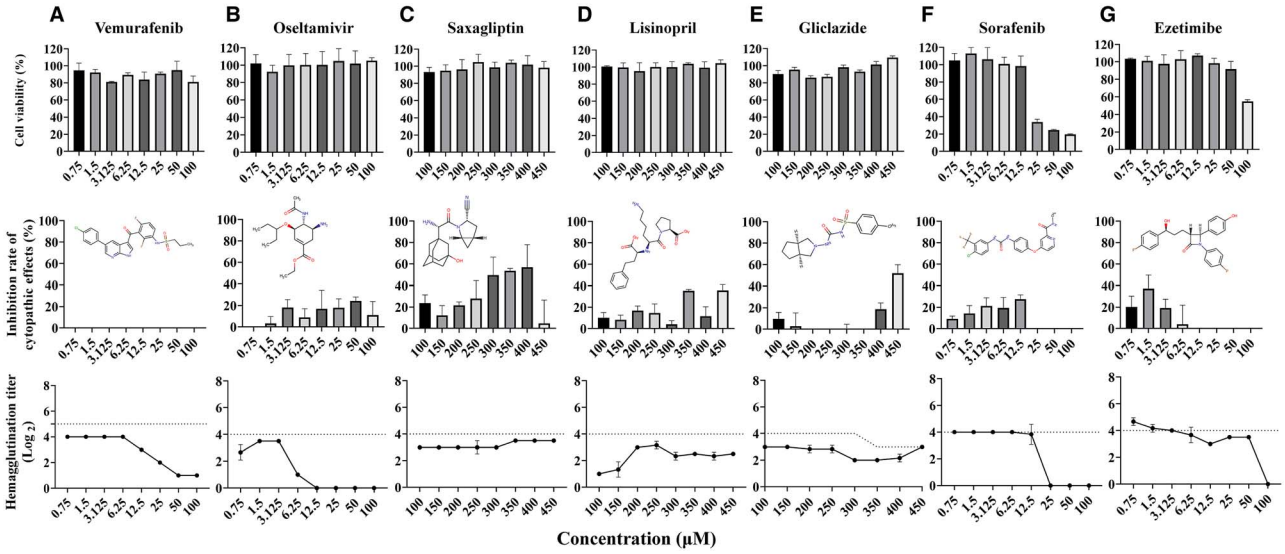

Figure 6. The verification of anti-IVA effect of candidates. The cytotoxicity (top), cytopathic effect inhibition (middle), and viral titer inhibition (bottom) capacities of two positive controls (A, B) and five candidates (C–G) were evaluated. The uninfected A549 cells treated with drugs were used to measure cytotoxicity. Cells exposed to PR8 H1N1 were employed to assess cytopathic effect inhibition. The corresponding culture supernatants were utilized to determine viral titer inhibition, and the dashed line represents the hemagglutination titer of the control sample without drug treatment. The data presented represent means ± SD from three independent replicates.

the anti-IVA effects of some drugs are unrelated to directly interacting host factors [63]. The underlying mechanisms may involve multiple signaling pathways processing and transmitting drug-target interaction signals. Therefore, integrating directional protein–protein interaction information with IVIPN will facilitate the exploration of how drug–target interaction signals are transduced to hub nodes and downstream metabolic activities.

This study introduces a dual-function workflow that combines exploration of influenza pathogenic mechanisms with the development of host-directed drugs. Further optimization includes the following steps. Firstly, Assigning PPI confidence scores to edges in IVIPNs will enhance the precision of causal relationship predictions. The edge weight is defined as $W = 1 - C$, where C represents the PPI confidence score from Human Integrated Protein-Protein Interaction rEference (HIPPIE) database [64] (ranging from 0 to 1). The strength of the causal relationship is determined by the total weight (W) of all PPIs involved, with a smaller sum indicating a stronger relationship. Secondly, the IVBOE reflects only the partial static synthesis process of influenza IVA viral particles, without considering the material and energy reserves required for viral lipid and protein modifications, as well as carbohydrate demands. Therefore, additional secondary equations responsible for details of viral replication are needed. The IVA's reliance on different objective equations during various replication stages can be represented by assigning varying weights. Thirdly, each IVIPN utilizes all HDIPs as causal nodes. This unbiased upper-level structure causes IVIPN to overlook dynamic changes in IVA–host protein interactions. It is crucial to note that IVA–host protein interactions in this study encompass not only the IVA's recognition of cell membrane surface receptors during infection but also various interactions within the cytoplasm. A single host cell may harbor IVAs at different life stages, suggesting the simultaneous occurrence of multiple IVA–host protein interactions within a cell. Therefore, additional prior knowledge is necessary to ascertain the predominant HDIPs at different stages. Fourthly, VIPNs reflected the regulation of metabolic flux through direct protein–protein interactions. Integrating VIPNs with transcriptional regulatory networks and metabolite–protein interaction networks will facilitate a systematic analysis of the effects of transcriptional regulation and metabolite feedback on metabolic flux. Lastly, due to the genetic and metabolic differences between A549 cells and normal epithelial cells, primary cells, and animal models are required for further evaluation of the antiviral efficacy of the candidate drugs. Antiviral strategies targeting host factors are often associated with substantial side effects [65], including disruptions to the metabolism of uninfected cells and potential off-target impacts on various tissues and organs [66]. Consequently, comprehensive assessments of the *in vivo* safety and tolerability of these candidates are imperative.

Conclusions

The study characterizes IVA-induced metabolic reprogramming via the IVBOEmodels, which integrate virus biomass equations and condition-specific transcriptomes. IVIPNs, protein networks derived from key metabolic enzymes and associated with host–virus interactions and metabolic reprogramming, feature infection-specific hub nodes. These hub nodes provide a rich array of potential host targets for drug repurposing. The efficacy of certain candidate drugs against IVA infection highlights the promising application of this research strategy in related studies of other infectious pathogens.

Materials and methods

Transcriptome data from infected cells and patients

The RNA-Seq data for human tracheobronchial epithelial (HTBE) cells infected with Influenza virus A/California/04/09 (H1N1) were selected from dataset GSE89008 [43] (Data ref: Heinz *et al.*, 2018). Gene expression was normalized to TPM (Transcripts Per Million) (Table S1). Microarray data for human whole blood cells infected with Influenza virus H1N1 were obtained from dataset GSE111368 [47] (Data ref: Dunning *et al.*, 2018) (Table S1). The details of sample selection and data processing are presented in File S1.

Interaction transcriptome and ribosome footprint data

Influenza–host interaction RNA-seq data (GSM2186929 [67] (Data ref: Bercovich-Kinori, Tai *et al.*, 2016), 8 hpi) and Influenza-host ribosome footprint Ribo-seq data (GSM2186925 [67] (Data ref: Bercovich-Kinori *et al.*, 2016), 8 hpi) were used to determine the TE of influenza virus proteins. The human reference genome (GRCh38), and the genome of influenza virus A/Puerto Rico/8/1934 (PR8, H1N1) (GCF_000865725.1) were used for data processing. The quantification of genes was presented as RPKM (Reads Per Kilobase of transcript per Million mapped reads) (SourceData S1). The details of data processing are presented in File S1.

Key human genes and interaction proteins related to influenza virus infection

A total of 14 202 unique key human genes related to influenza were collected from the database including DisGeNET [68], GeneCards [69], Comparative Toxicogenomics Database (CTD) [70], and relevant reference [71]. A total of 1292 unique human proteins directly interacting with influenza were collected from the study of Heaton *et al.* [72] and partial results reviewed by Watanabe *et al.* [73]. The details of data sources are presented in File S1.

Human protein–protein interaction network and drug–target interaction network

The complete human PPIN was extracted from the HIPPIE database [64]. A network containing 15 051 drug–target interactions was collected from the DrugBank database [57]. The details of network processing are shown in File S1.

Construction of the influenza virus A biomass equation

The genome of influenza virus A/Puerto Rico/8/1934 (PR8, H1N1) (GCF_000865725.1) was utilized for IVBOE construction by reported methods [34, 35].

The nucleotide composition in the IVBOE was determined by the total amount of four ribonucleotides from one copy of the genome −ssRNA and multiple copies of replication intermediates +ssRNA. Calculating the TE for each IVA protein provided the nucleotide requirements for all types of replication intermediates +ssRNA. A viral protein's TE is defined as the ratio of the RPKM from Ribo-seq to the RPKM from mRNA-seq [74] (Source Data S1).

The amino acid composition was determined by the copy number, amino acid composition, and molar mass of IVA proteins. The lipid composition was referred to as the Golgi membrane of host cells [34, 41]. The amount of ATP required and pyrophosphate released for synthesizing each viral particle is related to protein and RNA synthesis [34, 41]. The polymerization of an amino acid requires approximately four ATP molecules on average, while the polymerization of a nucleotide releases about one pyrophosphate on average [34, 41].

The methods for calculating biomass precursors, as well as the details of biomass equation assembly and integration, are shown in File S1. Parameters for calculating biomass precursors and the completed biomass equation are shown in Source Data S2.

Generation and differential flux analysis of condition-specific IVBOEmodels

Condition-specific IVBOEmodels were generated post-transcriptome constraint. The ftINIT algorithm was utilized to automatically generate personalized IVBOEmodels tailored for specific cell types [42]. Within the same group, the gene expression values of multiple samples were averaged and employed to constrain the original human GSMM (UImodels) consisting of 13 082 metabolic reactions and 8378 metabolites [75] or IVBOEmodels. The methodological details of flux sampling and differential flux analysis of the model are shown in File S1. Reactions with differential fluxes are presented in Source Data S3. The gene IDs of metabolic enzymes responsible for reactions with differential fluxes were selected based on the "Gene-Protein-Reaction" rules in UImodels and designated as the ERFs layer in IVIPNs.

Hypergeometric testing was used for enrichment analysis of metabolic subsystems that contained reactions with significantly different fluxes. The adjusted *P*-value was used to determine significantly enriched metabolic subsystems.

Construction of influenza virus A–induced protein networks

The IVA–induced protein networks (IVIPNs) consisted of three components. The first part comprised Host proteins Directly interacting with Influenza virus Proteins (HDIPs). The second part involved Enzymes responsible for Reactions with significantly different Fluxes (ERFs), identified via the aforementioned differential flux analysis. With the background of completed human PPIN, the function *all_shortest_paths* with a parameter "method = dijkstra" of the Python package NetworkX [76] was employed to extract the shortest protein paths between HDIPs and ERFs. These shortest paths established the causal relationships between HDIPs and ERFs and constituted the hidden layers of IVIPNs. Node information of temporal IVIPNs ($n = 5$) and stage-specific IVIPNs ($n = 3$) is presented in Source Data S4.

Identification of hub nodes related to influenza virus A infection

Eigenvector centrality, degree centrality, betweenness centrality, and Random Walk with Restart (RWR) were used to identify hub nodes in the IVIPNs (Source Data S5). The details of these algorithms are introduced in File S1.

The Python package NetworkX [76] was applied to implement the aforementioned algorithms. Nodes meeting the criteria for Eigenvector centrality, degree centrality, betweenness centrality, and Random Walk with Restart (RWR) with $P < .05$ are considered hub nodes.

Functional enrichment

The online tool Enrichr [77] was applied to the enrichment analysis of hidden layer proteins and hub nodes based on KEGG pathways and GO biological processes. Pathways with $q < 0.05$ were considered significantly enriched (Table S2).

Drug repurposing

A network-based proximity analysis [58] was conducted on the IVIPNs, and the details of it are introduced in File S1. Drugs with $Z < -1.5$ were considered to be highly relevant to influenza disease (Table S3).

Cell, virus, and reagents

A549 human lung carcinoma cells were purchased from the American Type Culture Collection (ATCC, VA, USA). Influenza virus A/Puerto Rico/8/1934 (PR8, H1N1) was kindly provided by Professor Hongbo Zhou from Huazhong Agricultural University, China. Five candidate drugs—saxagliptin hydrochloride, lisinopril dihydrate, sorafenib tosylate, ezetimibe, and gliclazide—along with

two positive controls, vemurafenib and oseltamivir phosphate, were purchased from Sigma-Aldrich (Sigma-Aldrich, MO, US). The details for cell culture, virus proliferation, and reagent usage are presented in File S1.

Detection of anti-influenza virus A infection capability

A549 cells were cultured overnight and digested with 0.25% trypsin (Gibco, CA, USA), then seeded into 96-well plates for 12 h in Dulbecco's Modified Eagle Medium (DMEM). For cytotoxicity testing, cells were washed and incubated in DMEM for 3 h. To evaluate the cytopathic effect inhibition, cells were infected with PR8 H1N1 (Multiplicity of Infection (MOI) = 0.001) for 3 h, followed by washing. Cells were cultured for 24 h in DMEM with 0.25 μg/ml L-(tosylamido-2-phenyl) ethyl chloromethyl ketone (TPCK)-treated trypsin (Sigma-Aldrich, MO, US), with or without candidate drugs (0.75–450 μM). Cytotoxicity and inhibition of the cytopathic effect were assessed using a CCK-8 assay. Hemagglutination assays with chicken red blood cells (CRBCs) determined PR8 titers, using serial dilutions of culture supernatants. Hemagglutination inhibition was indicated by the highest dilution preventing CRBC hemagglutination. The details of detections are presented in File S1.

Key Points

- Stage-specific metabolic reprogramming of host induced by influenza virus A (IVA) was depicted.
- genome-scale metabolic models capturing postinfection metabolic details were reconstructed with the IVA biomass equation.
- Hub nodes related to IVA infection were screened and applied to drug repurposing.
- Lisinopril, saxagliptin, and gliclazide were discovered with anti-IVA effects *in vitro*.

Acknowledgements

We appreciate Professor Hongbo Zhou's team for providing the viral strain and experimental guidance.

Author contributions

Conceptualization: Qingye Zhang; writing—original draft: Hao Tang; formal analysis: Feng Jiang; visualization: Feng Jiang; validation: Hao Tang, Zhi Zhang, Jiaojiao Yang; writing—review and editing: Qingye Zhang, Lu Li; funding acquisition: Qingye Zhang. All authors have read and agreed to the version of this manuscript.

Supplementary data

Supplementary data are available at *Briefings in Bioinformatics* online.

Funding

This work was supported by Fundamental Research Funds for the Central Universities (No. 2662024JC009, No. 2662022XXYJ007).

References

1. Focosi D, McConnell S, Shoham S. *et al.* Nirmatrelvir and COVID-19: Development, pharmacokinetics, clinical efficacy, resistance, relapse, and pharmacoeconomics. *Int J Antimicrob Agents* 2023;**61**:106708. https://doi.org/10.1016/j.ijantimicag.2022.106708.
2. Jones JC, Yen HL, Adams P. *et al.* Influenza antivirals and their role in pandemic preparedness. *Antivir Res* 2023;**210**:105499. https://doi.org/10.1016/j.antiviral.2022.105499.
3. Schalkwijk HH, Snoeck R, Andrei G. Acyclovir resistance in herpes simplex viruses: Prevalence and therapeutic alternatives. *Biochem Pharmacol* 2022;**206**:115322. https://doi.org/10.1016/j.bcp.2022.115322.
4. Wang R, Wang Z, Yuan H. *et al.* Mechanistic exploration of COVlD-19 antiviral drug ritonavir on anaerobic digestion through experimental validation coupled with metagenomics analysis. *J Hazard Mater* 2024;**479**:135603. https://doi.org/10.1016/j.jhazmat.2024.135603.
5. Li W, Wu J, Zhang J. *et al.* Puerarin-loaded PEG-PE micelles with enhanced anti-apoptotic effect and better pharmacokinetic profile. *Drug Deliv* 2018;**25**:827–37. https://doi.org/10.1080/10717544.2018.1455763.
6. Ruan Y, Yuan PP, Li PY. *et al.* Tingli Dazao Xiefei decoction ameliorates asthma in vivo and in vitro from lung to intestine by modifying NO-CO metabolic disorder mediated inflammation, immune imbalance, cellular barrier damage, oxidative stress and intestinal bacterial disorders. *J Ethnopharmacol* 2023;**313**:116503. https://doi.org/10.1016/j.jep.2023.116503.
7. Deng P, Dong X, Wu Z. *et al.* Development of glycosylation-modified (D)PPA-1 compounds as innovative PD-1/PD-L1 blockers: Design, synthesis, and biological evaluation. *Molecules* 2024;**29**:1898. https://doi.org/10.3390/molecules29081898.
8. Ianevski A, Ahmad S, Anunnitipat K. *et al.* Seven classes of antiviral agents. *Cell Mol Life Sci* 2022;**79**:605. https://doi.org/10.1007/s00018-022-04635-1.
9. Miller BE, Mistry S, Smart K. *et al.* The pharmacokinetics and pharmacodynamics of danirixin (GSK1325756)–a selective CXCR2 antagonist–in healthy adult subjects. *BMC Pharmacol Toxicol* 2015;**16**:18. https://doi.org/10.1186/s40360-015-0017-x.
10. Triana-Baltzer GB, Babizki M, Chan MC. *et al.* DAS181, a sialidase fusion protein, protects human airway epithelium against influenza virus infection: An in vitro pharmacodynamic analysis. *J Antimicrob Chemother* 2010;**65**:275–84. https://doi.org/10.1093/jac/dkp421.
11. Schor S, Einav S. Repurposing of kinase inhibitors as broad-Spectrum antiviral drugs. *DNA Cell Biol* 2018;**37**:63–9. https://doi.org/10.1089/dna.2017.4033.
12. Kumar N, Sharma S, Kumar R. *et al.* Host-directed antiviral therapy. *Clin Microbiol Rev* 2020;**33**:33. https://doi.org/10.1128/CMR.00168-19.
13. Hollenbaugh JA, Munger J, Kim B. Metabolite profiles of human immunodeficiency virus infected CD4+ T cells and macrophages using LC-MS/MS analysis. *Virology* 2011;**415**:153–9. https://doi.org/10.1016/j.virol.2011.04.007.
14. Yuan S, Chu H, Chan JF. *et al.* SREBP-dependent lipidomic reprogramming as a broad-spectrum antiviral target. *Nat Commun* 2019;**10**:120. https://doi.org/10.1038/s41467-018-08015-x.
15. Crater JM, Nixon DF, Furler O'Brien RL. HIV-1 replication and latency are balanced by mTOR-driven cell metabolism. *Front Cell Infect Microbiol* 2022;**12**:1068436. https://doi.org/10.3389/fcimb.2022.1068436.
16. Anders PM, Zhang Z, Bhende PM. *et al.* The KSHV K1 protein modulates AMPK function to enhance cell survival. *PLoS Pathog* 2016;**12**:e1005985. https://doi.org/10.1371/journal.ppat.1005985.

17. Clarke PR, Hardie DG. Regulation of HMG-CoA reductase: Identification of the site phosphorylated by the AMP-activated protein kinase in vitro and in intact rat liver. *EMBO J* 1990;**9**:2439–46. https://doi.org/10.1002/j.1460-2075.1990.tb07420.x.
18. Bultot L, Guigas B, Von Wilamowitz-Moellendorff A. *et al.* AMP-activated protein kinase phosphorylates and inactivates liver glycogen synthase. *Biochem J* 2012;**443**:193–203. https://doi.org/10.1042/BJ20112026.
19. Huttlin EL, Bruckner RJ, Navarrete-Perea J. *et al.* Dual proteome-scale networks reveal cell-specific remodeling of the human interactome. *Cell* 2021;**184**:3022–3040.e3028. https://doi.org/10.1016/j.cell.2021.04.011.
20. Scheffner M, Huibregtse JM, Vierstra RD. *et al.* The HPV-16 E6 and E6-AP complex functions as a ubiquitin-protein ligase in the ubiquitination of p53. *Cell* 1993;**75**:495–505. https://doi.org/10.1016/0092-8674(93)90384-3.
21. Martinez-Zapien D, Ruiz FX, Poirson J. *et al.* Structure of the E6/E6AP/p53 complex required for HPV-mediated degradation of p53. *Nature* 2016;**529**:541–5. https://doi.org/10.1038/nature16481.
22. Jiang P, Du W, Wang X. *et al.* p53 regulates biosynthesis through direct inactivation of glucose-6-phosphate dehydrogenase. *Nat Cell Biol* 2011;**13**:310–6. https://doi.org/10.1038/ncb2172.
23. Zwerschke W, Mazurek S, Massimi P. *et al.* Modulation of type M2 pyruvate kinase activity by the human papillomavirus type 16 E7 oncoprotein. *Proc Natl Acad Sci USA* 1999;**96**:1291–6. https://doi.org/10.1073/pnas.96.4.1291.
24. Wu YH, Yang Y, Chen CH. *et al.* Aerobic glycolysis supports hepatitis B virus protein synthesis through interaction between viral surface antigen and pyruvate kinase isoform M2. *PLoS Pathog* 2021;**17**:e1008866. https://doi.org/10.1371/journal.ppat.1008866.
25. Yue M, Hu B, Li J. *et al.* Coronaviral ORF6 protein mediates inter-organelle contacts and modulates host cell lipid flux for virus production. *EMBO J* 2023;**42**:e112542. https://doi.org/10.15252/embj.2022112542.
26. Ramière C, Rodriguez J, Enache LS. *et al.* Activity of hexokinase is increased by its interaction with hepatitis C virus protein NS5A. *J Virol* 2014;**88**:3246–54. https://doi.org/10.1128/JVI.02862-13.
27. Mosharaf MP, Alam K, Gow J. *et al.* Exploration of key drug target proteins highlighting their related regulatory molecules, functional pathways and drug candidates associated with delirium: Evidence from meta-data analyses. *BMC Geriatr* 2023;**23**:767.
28. Emad A, Cairns J, Kalari KR. *et al.* Knowledge-guided gene prioritization reveals new insights into the mechanisms of chemoresistance. *Genome Biol* 2017;**18**:153. https://doi.org/10.1186/s13059-017-1282-3.
29. Xu J, Mao C, Hou Y. *et al.* Interpretable deep learning translation of GWAS and multi-omics findings to identify pathobiology and drug repurposing in Alzheimer's disease. *Cell Rep* 2022;**41**:111717. https://doi.org/10.1016/j.celrep.2022.111717.
30. Han N, Hwang W, Tzelepis K. *et al.* Identification of SARS-CoV-2-induced pathways reveals drug repurposing strategies. *Sci Adv* 2021;**7**:7. https://doi.org/10.1126/sciadv.abh3032.
31. Palmer CS. Innate metabolic responses against viral infections. *Nat Metab* 2022;**4**:1245–59. https://doi.org/10.1038/s42255-022-00652-3.
32. Lin J, Wang L, Huang M. *et al.* Metabolic changes induced by heavy metal copper exposure in human ovarian granulosa cells. *Ecotoxicol Environ Saf* 2024;**285**:117078. https://doi.org/10.1016/j.ecoenv.2024.117078.
33. Ye C, Wei X, Shi T. *et al.* Genome-scale metabolic network models: From first-generation to next-generation. *Appl Microbiol Biotechnol* 2022;**106**:4907–20. https://doi.org/10.1007/s00253-022-12066-y.
34. Nanda P, Ghosh A. Genome scale-differential flux analysis reveals deregulation of lung cell metabolism on SARS-CoV-2 infection. *PLoS Comput Biol* 2021;**17**:e1008860. https://doi.org/10.1371/journal.pcbi.1008860.
35. Aller S, Scott A, Sarkar-Tyson M., Soyer OS In: Cogdell R (ed.), *Integrated Human-Virus Metabolic Stoichiometric Modelling Predicts Host-Based Antiviral Targets against Chikungunya*. Dengue and Zika viruses: J R Soc Interface, 2018. 20180125, **15**. 10.1098/rsif.2018.0125.
36. Monto AS, Fukuda K. Lessons from influenza pandemics of the last 100 years. *Clin Infect Dis* 2020;**70**:951–7. https://doi.org/10.1093/cid/ciz803.
37. Uyeki TM, Hui DS, Zambon M. *et al.* Influenza. *Lancet* 2022;**400**:693–706. https://doi.org/10.1016/S0140-6736(22)00982-5.
38. Aguirre J, Guantes R. Virus-host protein co-expression networks reveal temporal organization and strategies of viral infection. *iScience* 2023;**26**:108475. https://doi.org/10.1016/j.isci.2023.108475.
39. Bösl K, Ianevski A, Than TT. *et al.* Common nodes of virus-host interaction revealed through an integrated network analysis. *Front Immunol* 2019;**10**:2186. https://doi.org/10.3389/fimmu.2019.02186.
40. Liu X, Huuskonen S, Laitinen T. *et al.* SARS-CoV-2-host proteome interactions for antiviral drug discovery. *Mol Syst Biol* 2021;**17**:e10396. https://doi.org/10.15252/msb.202110396.
41. van Meer G. Lipids of the Golgi membrane. *Trends Cell Biol* 1998;**8**:29–33. https://doi.org/10.1016/s0962-8924(97)01196-3.
42. Gustafsson J, Anton M, Roshanzamir F. *et al.* Generation and analysis of context-specific genome-scale metabolic models derived from single-cell RNA-Seq data. *Proc Natl Acad Sci USA* 2023;**120**:e2217868120. https://doi.org/10.1073/pnas.2217868120.
43. Heinz S, Texari L, Hayes MGB. *et al.* Transcription elongation can affect genome 3D structure. *Cell* 2018;**174**:1522–1536.e1522. https://doi.org/10.1016/j.cell.2018.07.047.
44. Limsuwat N, Boonarkart C, Phakaratsakul S. *et al.* Influence of cellular lipid content on influenza a virus replication. *Arch Virol* 2020;**165**:1151–61. https://doi.org/10.1007/s00705-020-04596-5.
45. Munshi SU, Taneja S, Bhavesh NS. *et al.* Metabonomic analysis of hepatitis E patients shows deregulated metabolic cycles and abnormalities in amino acid metabolism. *J Viral Hepat* 2011;**18**:e591–602. https://doi.org/10.1111/j.1365-2893.2011.01488.x.
46. Brito CVB, Rodrigues ÉDL, Martins FMS. *et al.* Immunological impact of tetrahydrobiopterin on the central nervous system in a murine model of rabies virus infection. *Rev Inst Med Trop Sao Paulo* 2021;**63**:e28. https://doi.org/10.1590/s1678-9946202163028.
47. Dunning J, Blankley S, Hoang LT. *et al.* Progression of whole-blood transcriptional signatures from interferon-induced to neutrophil-associated patterns in severe influenza. *Nat Immunol* 2018;**19**:625–35. https://doi.org/10.1038/s41590-018-0111-5.
48. Zotenko E, Mestre J, O'Leary DP. *et al.* Why do hubs in the yeast protein interaction network tend to be essential: Reexamining the connection between the network topology and essentiality. *PLoS Comput Biol* 2008;**4**:e1000140. https://doi.org/10.1371/journal.pcbi.1000140.
49. Wang X, Tan J, Zoueva O. *et al.* Novel pandemic influenza a (H1N1) virus infection modulates apoptotic pathways that impact its replication in A549 cells. *Microbes Infect* 2014;**16**:178–86. https://doi.org/10.1016/j.micinf.2013.11.003.

50. Alon R, Sportiello M, Kozlovski S. *et al.* Leukocyte trafficking to the lungs and beyond: Lessons from influenza for COVID-19. *Nat Rev Immunol* 2021;**21**:49–64. https://doi.org/10.1038/s41577-020-00470-2.
51. Londino JD, Lazrak A, Collawn JF. *et al.* Influenza virus infection alters ion channel function of airway and alveolar cells: Mechanisms and physiological sequelae. *Am J Physiol Lung Cell Mol Physiol* 2017;**313**:L845–l858. https://doi.org/10.1152/ajplung.00244.2017.
52. Skehel JJ, Wiley DC. Receptor binding and membrane fusion in virus entry: The influenza hemagglutinin. *Annu Rev Biochem* 2000;**69**:531–69. https://doi.org/10.1146/annurev.biochem.69.1.531.
53. Tran V, Ledwith MP, Thamamongood T. *et al.* Influenza virus repurposes the antiviral protein IFIT2 to promote translation of viral mRNAs. *Nat Microbiol* 2020;**5**:1490–503. https://doi.org/10.1038/s41564-020-0778-x.
54. Park ES, Dezhbord M, Lee AR. *et al.* The roles of ubiquitination in pathogenesis of influenza virus infection. *Int J Mol Sci* 2022;**23**:4593.
55. Lowy RJ. Influenza virus induction of apoptosis by intrinsic and extrinsic mechanisms. *Int Rev Immunol* 2003;**22**:425–49. https://doi.org/10.1080/08830180305216.
56. Lin X, Wang R, Zou W. *et al.* The influenza virus H5N1 infection can induce ROS production for viral replication and host cell death in A549 cells modulated by human Cu/Zn superoxide dismutase (SOD1) overexpression. *Viruses* 2016;**8**:8. https://doi.org/10.3390/v8010013.
57. Knox C, Wilson M, Klinger CM. *et al.* DrugBank 6.0: The DrugBank knowledgebase for 2024. *Nucleic Acids Res* 2024;**52**:D1265–d1275. https://doi.org/10.1093/nar/gkad976.
58. Guney E, Menche J, Vidal M. *et al.* Network-based in silico drug efficacy screening. *Nat Commun* 2016;**7**:10331. 10.1038/ncomms10331.
59. Lu X, Tang X, Guo W. *et al.* Sorafenib induces growth inhibition and apoptosis of human chondrosarcoma cells by blocking the RAF/ERK/MEK pathway. *J Surg Oncol* 2010;**102**:821–6. https://doi.org/10.1002/jso.21661.
60. Pleschka S, Wolff T, Ehrhardt C. *et al.* Influenza virus propagation is impaired by inhibition of the Raf/MEK/ERK signalling cascade. *Nat Cell Biol* 2001;**3**:301–5. https://doi.org/10.1038/35060098.
61. Mamputu JC, Renier G. Advanced glycation end products increase, through a protein kinase C-dependent pathway, vascular endothelial growth factor expression in retinal endothelial cells. Inhibitory effect of gliclazide. *J Diabetes Complications* 2002;**16**:284–93.
62. Bautista E, Arcos M, Jimenez-Alvarez L. *et al.* Angiogenic and inflammatory markers in acute respiratory distress syndrome and renal injury associated to A/H1N1 virus infection. *Exp Mol Pathol* 2013;**94**:486–92. https://doi.org/10.1016/j.yexmp.2013.03.007.
63. Holzberg M, Boergeling Y, Schräder T. *et al.* Vemurafenib limits influenza a virus propagation by targeting multiple signaling pathways. *Front Microbiol* 2017;**8**:2426.
64. Alanis-Lobato G, Andrade-Navarro MA, Schaefer MH. HIPPIE v2.0: Enhancing meaningfulness and reliability of protein-protein interaction networks. *Nucleic Acids Res* 2017;**45**:D408–d414. https://doi.org/10.1093/nar/gkw985.
65. Geraghty RJ, Aliota MT. In: Lin C-W (ed.), *Bonnac LF*. Broad-Spectrum Antiviral Strategies and Nucleoside Analogues: Viruses, 2021, 13.
66. Cheney L, Barbaro JM, Berman JW. In: Münz C (ed.), *Berman JW*. Antiretroviral Drugs Impact Autophagy with Toxic Outcomes: Cells, 2021. 10, **10**. 10.3390/cells10040909.
67. Bercovich-Kinori A, Tai J, Gelbart IA. *et al.* A systematic view on influenza induced host shutoff. *elife* 2016;**5**:5. https://doi.org/10.7554/eLife.18311.
68. Piñero J, Ramírez-Anguita JM, Saüch-Pitarch J. *et al.* The DisGeNET knowledge platform for disease genomics: 2019 update. *Nucleic Acids Res* 2020;**48**:D845–d855. https://doi.org/10.1093/nar/gkz1021.
69. Stelzer G, Rosen N, Plaschkes I. *et al.* The GeneCards suite: From gene data mining to disease genome sequence analyses. *Curr Protoc Bioinformatics* 2016;**54**:1.30.1–1.30.33. https://doi.org/10.1002/cpbi.5.
70. Davis AP, Grondin CJ, Johnson RJ. *et al.* Comparative Toxicogenomics database (CTD): Update 2021. *Nucleic Acids Res* 2021;**49**:D1138–d1143. https://doi.org/10.1093/nar/gkaa891.
71. Eliopoulos AG, Angelis A, Liakakou A. *et al.* Vitro anti-influenza virus activity of non-polar Primula veris subsp. veris extract. *Pharmaceuticals (Basel)* 2022;**15**:1513. https://doi.org/10.3389/fnut.2025.1524125.
72. Heaton NS, Moshkina N, Fenouil R. *et al.* Targeting viral Proteostasis limits influenza virus, HIV, and dengue virus infection. *Immunity* 2016;**44**:46–58. https://doi.org/10.1016/j.immuni.2015.12.017.
73. Watanabe T, Watanabe S, Kawaoka Y. Cellular networks involved in the influenza virus life cycle. *Cell Host Microbe* 2010;**7**:427–39. https://doi.org/10.1016/j.chom.2010.05.008.
74. Ingolia NT, Ghaemmaghami S, Newman JR. *et al.* Genome-wide analysis in vivo of translation with nucleotide resolution using ribosome profiling. *Science* 2009;**324**:218–23. https://doi.org/10.1126/science.1168978.
75. Robinson JL, Kocabaş P, Wang H. *et al.* An atlas of human metabolism. *Sci Signal* 2020;**13**:13. https://doi.org/10.1126/scisignal.aaz1482.
76. Hagberg A, Swart PJ, Schult DA. In: Kurths J (ed.), *Exploring Network Structure, Dynamics, and Function Using NetworkX. Los Alamos National Laboratory (LANL)*. Los Alamos, NM (United States), 2008. https://doi.org/10.1063/1.2975842.
77. Xie Z, Bailey A, Kuleshov MV. *et al.* Gene set knowledge discovery with Enrichr. *Curr Protoc* 2021;**1**:e90. https://doi.org/10.1002/cpz1.90.

Briefings in Bioinformatics, 2025, **26(3)**, bbaf163
https://doi.org/10.1093/bib/bbaf163
Case Study